Facile Fabrication of Superhydrophobic Paper with Excellent Water Repellency and Moisture Resistance by Phase Separation

Pan Li, Hui Li,* Jin Yang, and Yahong Meng

A simple but effective method of fabricating superhydrophobic paper with excellent moisture resistance was developed by precipitating carnauba wax onto the surface of cellulose fibers using a phase separation method. Response surface methodology (RSM) was used to optimize the effects of the preparation variables on the water contact angle (WCA) of the paper surface. The four independent variables were carnauba wax concentration, immersion time, coagulation bath ratio (water/ethanol), and coagulation bath time. The optimal treatment conditions were as follows: wax concentration, 3.78% (wax/chloroform, w/v); immersion time, 1.46 h; coagulation bath ratio, 13/87 (water/ethanol, v/v); and coagulation bath time, 2.63 h. Under these conditions, the experimental WCA reached 152.7°, which agreed closely with the predicted value of 154.1°. The surface morphology of the superhydrophobic paper was characterized by scanning electron microscopy (SEM) and atomic force microscopy (AFM), and the images showed that cluster-like carnauba wax aggregation completely covered the fiber surface, resulting in increased roughness. Moreover, the moisture resistance of the obtained superhydrophobic paper was evaluated. The results demonstrated that under high relative humidity conditions, the moisture resistance of the superhydrophobic paper significantly improved, and its tensile strength remained high.

Keywords: Superhydrophobicity; Carnauba wax; Phase separation; Moisture resistance; Response surface methodology

*Contact information: Research Institute of Food Safety, Kunming University of Science and Technology, Kunming 650600, China; *Corresponding author: lihuiscut@126.com*

INTRODUCTION

Paper is composed mainly of fibrous cellulose, and it is a common and essential material with many virtues. It is low-cost, renewable, and biodegradable, with good mechanical properties (Geissler *et al*. 2014). The main weakness of paper, especially compared to plastics, is its highly hydrophilic character, which is due to the many active hydroxyl groups of the structural polysaccharide cellulose (Ogihara *et al*. 2012). Paper with water-repellent properties can be useful in various fields, such as waterproof books or journals, beverage packaging, microfluidic devices, and lab-on-paper devices (Tang *et al*. 2013; Elsharkawy *et al*. 2014). Therefore, the creation of hydrophobic paper has both academic and practical potential, particularly with the recent rising interest in superhydrophobic paper (Sousa and Mano 2013).

Although various methods that are used to prepare superhydrophobic material surfaces, such as the sol-gel method (Shi *et al*. 2012), chemical vapor deposition (Crick *et al*. 2012), and ink-jet printing (Zhang *et al*. 2015), have been closely studied, research on

superhydrophobic cellulose fiber-based products is limited because most of these methods cannot simply be applied to cellulose fiber-based paper without compromising efficiency. A number of approaches, including chemical grafting modification (Bongiovanni *et al*. 2013), spray coating (Ogihara *et al*. 2012), the rapid expansion of supercritical CO_2 (Werner *et al.* 2010), and plasma treatment (Balu *et al.* 2008) have been reported as means of preparing superhydrophobic cellulose fiber-based materials, but these techniques have several limitations, such as requiring specialized and costly instrumentation, employing tedious fabrication procedures, and having low grafting efficiency (Huang *et al.* 2011). Other approaches for imparting superhydrophobicity to paper, such as multilayer deposition of polydiallyldimethylammonium chloride and silica particles, followed by a chemical modification with fluoroalkylsilane, have been reported (Yang and Deng 2008; Zhang *et al.* 2012). However, some drawbacks still exist; for example, fluoroalkylsilanes are high in cost and pose potential risks for human and environmental health (Li *et al.* 2008).

Phase separation is a relatively facile, efficient, and low-cost method of attaining a superhydrophobic surface, and it can be applied to the preparation superhydrophobic paper. Obeso *et al.* (2013) fabricated a biomimetic superhydrophobic paper through precipitation of poly(hydroxybutyrate) (PHB) on the surface of cellulose fibers using a phase separation process. PHBs are an attractive potential substitute for petroleum-derived synthetic plastics; however, high production costs make these polymers commercially uncompetitive (Pradella *et al.* 2012). Carnauba wax, made from the leaves of the Brazilian palm (*Copernica cerifera*), is low-cost, and possesses nontoxicity and moisture barrier characteristics, for which reason it is commonly used as a fruit coating to prevent moisture loss and extend shelf-life (Barman *et al.* 2011). In this study, the phase separation method was used to fabricate superhydrophobic paper, and the paper surface was modified through precipitation of a coating of carnauba wax. The processing parameters for the phase separation were optimized using response surface methodology. The surface wetting property of the obtained paper was investigated using a water contact angle measurement. The surface morphology of the obtained superhydrophobic paper was characterized by scanning electron microscopy (SEM) and atomic force microscopy (AFM). In addition, the moisture resistance of the resulting superhydrophobic paper was studied.

EXPERIMENTAL

Materials

The filter papers used as the supporting substrate were purchased from Hangzhou Special Paper Co., Ltd (Hangzhou, China). Natural plant carnauba wax with a melting point of 82.5 °C was purchased from the Shanghai Aladdin Reagent Co., Ltd (Shanghai, China). Chloroform and ethanol, of 99% and 99.5% purity, were purchased from Chongqing Chuandong Chemical Engineering Co., Ltd. (Chongqing, China). Milli-Q water (Millipore, Billerica, MA, USA) with a resistivity of 18 MΩ/cm was used in all experiments. All chemicals were used as received without further purification.

Preparation of Superhydrophobic Paper

Before use, the filter papers were cut into strips of size 150 mm × 15 mm. The strips were first immersed in a 1 to 11% (w/v) solution of carnauba wax in chloroform for 1 to 6

h at 50 °C, followed by immersion in a coagulation bath composed of a mixture of water and ethanol for 1 to 6 h at room temperature. Finally, the strips were placed on a glass surface and dried at room temperature.

Experimental Design

Single factor experiments

The effects of four factors, namely carnauba wax concentration, immersion time, coagulation bath ratio, and coagulation bath time, on the paper hydrophobicity were studied using a single factor design. Specifically, the single factor experiment was performed at a designated carnauba wax concentration between 1 and 11% (w/v), immersion time from 1 to 6 h, coagulation bath ratio from 35/65 to 10/90 (water/ethanol, v/v), and coagulation bath time from 1 to 6 h.

In each experiment, one factor was changed, while the other factors were kept constant. The effect of each factor was evaluated by determining the water contact angle (WCA) of the paper.

Optimization of process conditions by Box-Behnken design (BBD)

On the basis of the single-factor experiment results, the ranges of each factor were confirmed, and then a four-variable (X_1, carnauba wax concentration; X_2, immersion time; X_3, coagulation bath ratio; X_4, coagulation bath time), three-level Box-Behnken Design (BBD) was used to evaluate the best conditions for the hydrophobic modification of paper. For statistical calculations, the variables were coded in the following Eq. 1,

$$X_i = (x_i - x_0)/\Delta x \quad (1)$$

where X_i is the coded value of the independent variable, x_i is the actual value of the independent variable, x_0 is the actual value of the independent variable at the center point, and Δx is the step change value. The range of independent variables and their levels are presented in Table 1.

The experimental runs for the BBD are shown in Table 2. Each experimental run was performed at least five times, and the averages of the WCA were taken as the response. The analysis of variance (ANOVA) of the quadratic regression model was conducted using Minitab15 (State College, PA, USA), and the response surface analyses were plotted using Design Expert software (Matlab, MathWorks, Natick, MA, USA).

Table 1. Independent Variables and their Levels in Box-Behnken Design

Independent Variables	Symbol		Level		
	Real	Coded	-1	0	1
Wax concentration (w/v)	x_1	X_1	1	3	5
Immerse time (h)	x_2	X_2	1	2	3
Coagulation bath ratio (water/ethanol, v/v)	x_3	X_3	20:80	15:85	10:90
Coagulation bath time (h)	x_4	X_4	2	3	4

Table 2. Box-Behnken Experimental Design and Results for WCA of Treated Paper

Run Number	Coded Variable Levels				WCA (°)
	X_1	X_2	X_3	X_4	
1	0	0	-1	-1	145.66
2	1	0	0	1	138.95
3	-1	0	1	0	105.95
4	0	-1	-1	0	149.26
5	-1	-1	0	0	98.21
6	-1	1	0	0	97.82
7	1	-1	0	0	145.24
8	0	0	-1	1	148.53
9	-1	0	0	1	98.98
10	0	0	0	0	150.9
11	0	1	0	1	141.33
12	-1	0	-1	0	92.12
13	0	1	0	-1	146.82
14	1	0	1	0	142.94
15	0	-1	1	0	150.61
16	1	0	-1	0	143.39
17	1	1	0	0	139.24
18	-1	0	0	-1	95.81
19	0	0	0	0	150.05
20	0	0	0	0	151.32
21	0	-1	0	1	148.82
22	0	1	1	0	145.36
23	0	1	-1	0	144.58
24	1	0	0	-1	145.46
25	0	0	1	-1	150.12
26	0	-1	0	-1	149.27
27	0	0	1	1	148.19

Surface Characterization

The surface morphology of the obtained superhydrophobic paper was observed using SEM (VEGA 3 SBH, Tescan, Brno, Czech Republic) and tapping mode AFM (Nanoscope IIIa Multimode, Veeco Co., Santa Barbara, CA, USA), with software version 5.12r3 (Veeco Co.) for AFM image offline data analysis. No image processing except flattening was made for the AFM image. At least five different spots from the same sample were scanned, and only images with reproducible features were reported.

Water contact angles were measured using a SL200B optical contact angle meter (Kino USA industry Co., Ltd, Chino, CA, USA) at ambient temperatures. Each pure water droplet (3 μL) was gently deposited on the testing surface using a microsyringe, and data were averaged from the measurements of at least five different positions for each sample.

Moisture Resistance Testing

A moisture resistance test was performed as described by Yang and Deng (2008). A high-humidity environment was prepared using a seal dryer. A strength-testing machine (DCP-KZ 300, Sichuan Changjiang Paper Instrument Co., Yibin, China) was employed to measure the tensile strength of the samples under different humidity conditions. All

samples were cut into specimens of 15 mm (width) × 150 mm (length) before the tensile strength measurements.

RESULTS AND DISCUSSION

Single Factor Experimental Analysis

When the paper strips are immersed in a coagulation bath, a separation into two phases occurs: a wax-rich phase and a wax-poor phase (Yuan *et al*. 2007; Oliveira *et al*. 2010). As chloroform and ethanol are miscible, the solvent in the wax solution is exchanged by the non-solvent (ethanol), and the wax precipitation is able to occur (Witte *et al*. 1996). Consequently, in the wax-poor phase, the wax nuclei are generated by precipitation. In the wax-rich phase, aggregates form around these nuclei in order to decrease the surface energy (Aruna *et al*. 2012). The carnauba wax concentration, immersion time, coagulation-bath ratio, and coagulation bath time were investigated, and the results of the single factor experiments are presented in Fig. 1.

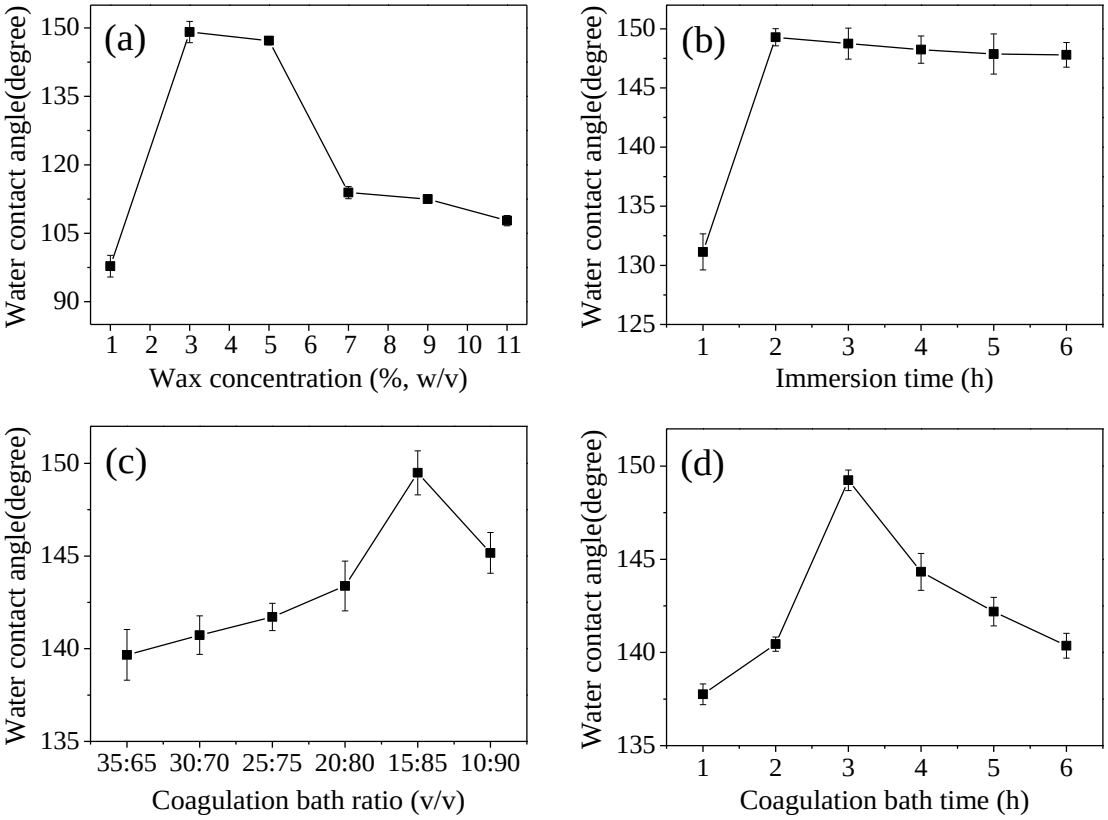

Fig. 1. Effects of the (a) concentration ratio, (b) immersion time, (c) coagulation bath ratio, and (d) coagulation bath time on the water contact angle of paper

Effect of carnauba wax concentration on water contact angle

In this trial, the carnauba wax concentrations were set at 1%, 3%, 5%, 7%, and 11% (w/v), while the other parameters were set as follows: immersion time, 2 h; coagulation bath ratio, 15:85 (v/v); and coagulation bath time, 3 h. As shown in Fig. 1a, as the carnauba wax concentration increased, the WCA of the paper surface increased initially and then

decreased. When the carnauba wax concentration was 3% (w/v), the surface showed the highest WCA of 149.1°. With further increases in concentration, the paper hydrophobicity began to decline. This result was attributed to the greater amounts of wax, generated during the wax-rich phase, which aggregated around the polymer nuclei that were generated by precipitation during the wax-poor phase. These wax aggregations resulted in flatter and more compact surface morphology of the wax coating on the cellulose fiber surface.

Effect of immersion time on water contact angle

In this trial, the immersion times were set at 1, 2, 3, 4, 5, and 6 h, while the other parameters were set as follows: wax concentration, 3% (w/v); coagulation bath ratio, 15:85; (v/v); and coagulation bath time, 3 h. As shown in Fig. 1b, the water contact angle increased with the increasing immersion time, indicating that a longer immersion time had a positive effect on the paper hydrophobicity. This result might have been due to the time requirement for the penetration and precipitation of the carnauba wax into the paper fiber network. Beyond 2 h, a longer immersion time resulted in a slightly increased hydrophobicity, which indicated that the precipitation of carnauba wax onto the paper fiber network had started due to the need to maintain a dynamic equilibrium with the increasing immersion time.

Effect of coagulation bath ratio on water contact angle

In this trial, the coagulation bath ratios were set at 35:65, 30:70, 25:75, 20:80, 15:85, and 10:90 (v/v), while the other parameters were set as follows: wax concentration, 3% (w/v); immersion time, 2 h; and coagulation bath time, 3 h. As shown in Fig. 1c, the water contact angle increased dramatically when the volume ratio of ethanol in the water/ethanol mixtures increased from 65% to 85%, and it reached a peak value of 149.5°. The positive effect of the high volume ratio of ethanol in the mixture was attributed to the fact that more wax nuclei were quickly generated during the wax precipitation in the wax-poor phase, resulting in rougher surface morphology of the wax coating. Furthermore, the water contact angle decreased when the volume ratio of ethanol continued to increase. A possible explanation for this is that the excessive wax nuclei that were formed in the wax-poor phase led to a flatter and more compact wax coating surface. Here, due to the low miscibility between the chloroform and the water, the presence of water in the coagulation bath served as a selective barrier, preventing the carnauba wax from spreading off the paper.

Effect of coagulation bath time on water contact angle

In this trial, the coagulation bath times were set at 1, 2, 3, 4, 5, and 6 h, while the other parameters were set as follows: wax concentration, 3% (w/v); immersion time, 2 h; and coagulation bath ratio, 15:85 (v/v). As shown in Fig. 1d, the water contact angle increased with increasing coagulation bath time, and the highest water contact angle value was obtained at the time of 3 h. However, after 3 h, the water contact angle decreased. This result suggests that the longer coagulation bath time led to flat surface morphology of the wax coating.

Response Surface Analysis

On the basis of the analyses of the single-factor experiments, the wax concentration, immersion time, coagulation bath ratio, and coagulation bath time were further optimized by employing a BBD experiment and RSM analysis. The BBD matrix and the WCA under different experimental conditions are shown in Table 2. The experimental data were

analyzed by multiple regression analysis using the Minitab 15 (Minitab Inc. 2007, State College, PA, USA), and a quadratic polynomial equation between WCA and the preparation variables was derived as follows,

$$Y = 150.76 + 22.19X_1 - 2.19X_2 + 1.64X_3 - 0.70X_4 - 28.73X_1^2 - 2.17X_2^2 - 0.90X_3^2 - 2.00X_4^2 - 1.40X_1X_2 - 3.57X_1X_3 - 2.42X_1X_4 - 0.14X_2X_3 - 1.26X_2X_4 - 1.20X_3X_4$$

where Y was the WCA of the obtained paper, and X_1, X_2, X_3, and X_4 were the coded values of the wax concentration ratio, immersion time, coagulation bath ratio, and coagulation bath time, respectively.

Table 3 shows the summary of analysis of variance (ANOVA) of the quadratic regression model, which consists of DF (the degree of freedom), Seq SS (sequential sum of squares), Adj SS(adjusted determination coefficient sum of squares), Adj MS(adjusted determination coefficient mean of square), *F*-value (the ratio of the regression mean square to the error mean square), and *P*-value. The *F*-value of this quadratic polynomial model was 341.2, while the corresponding *P*-value was less than 0.0001, which implied the model was statistically significant and represented the real relationship among the variables. The *F*-value of 6.55 and *P*-value of 0.140 for lack-of-fit implied that the lack-of-fit was not significant relative to the pure error, indicating that the model equation was adequate for predicting the WCA of the obtained paper within the range of the experimental variables. In addition, the determination coefficient (R^2) of the model was 0.9975, indicating that 99.75% of the variability in the WCA response could be explained by the model and by the close agreement between the experimental and predicted values of the WCA. The multiple adjusted determination coefficient (Adj R^2), an alternative measure of model adequacy, was 0.9946, meaning that 99.46% of the total variation was explained by the model, which suggests that the polynomial model equation had a high-quality fit of good precision and reliability.

Table 3. ANOVA for the Regression Model

Source	DF	Seq SS	Adj SS	Adj MS	*F*-value	*P*-value
Model	14	11255.5	11255.53	803.97	341.25	0.000
Linear	4	6006.3	6006.35	1501.59	637.36	0.000
Square	4	5154.7	5154.72	1288.68	546.99	0.000
Interaction	6	94.5	94.46	15.74	6.68	0.003
Residual	12	28.3	28.27	2.36		
Lack-of-fit	10	27.4	27.43	2.74	6.55	0.140
Pure error	2	0.8	0.84	0.42		
Total	26	11283.8				
R^2 = 99.75% ; R^2_{Adj} = 99.46%						

Furthermore, the significance of each regression coefficient in the quadratic polynomial equation was also analyzed, and the results are listed in Table 4. The variables with extremely significant ($P < 0.01$) effects on the WCA of paper were the linear terms (X_1, X_2 and X_3), the quadratic terms ($X_1 \times X_1$ and $X_1 \times X_1$), and the interaction terms ($X_1 \times X_3$

and $X_1 \times X_4$). The quadratic term ($X_4 \times X_4$) was significant ($P < 0.05$). The other terms were not significant ($P > 0.05$).

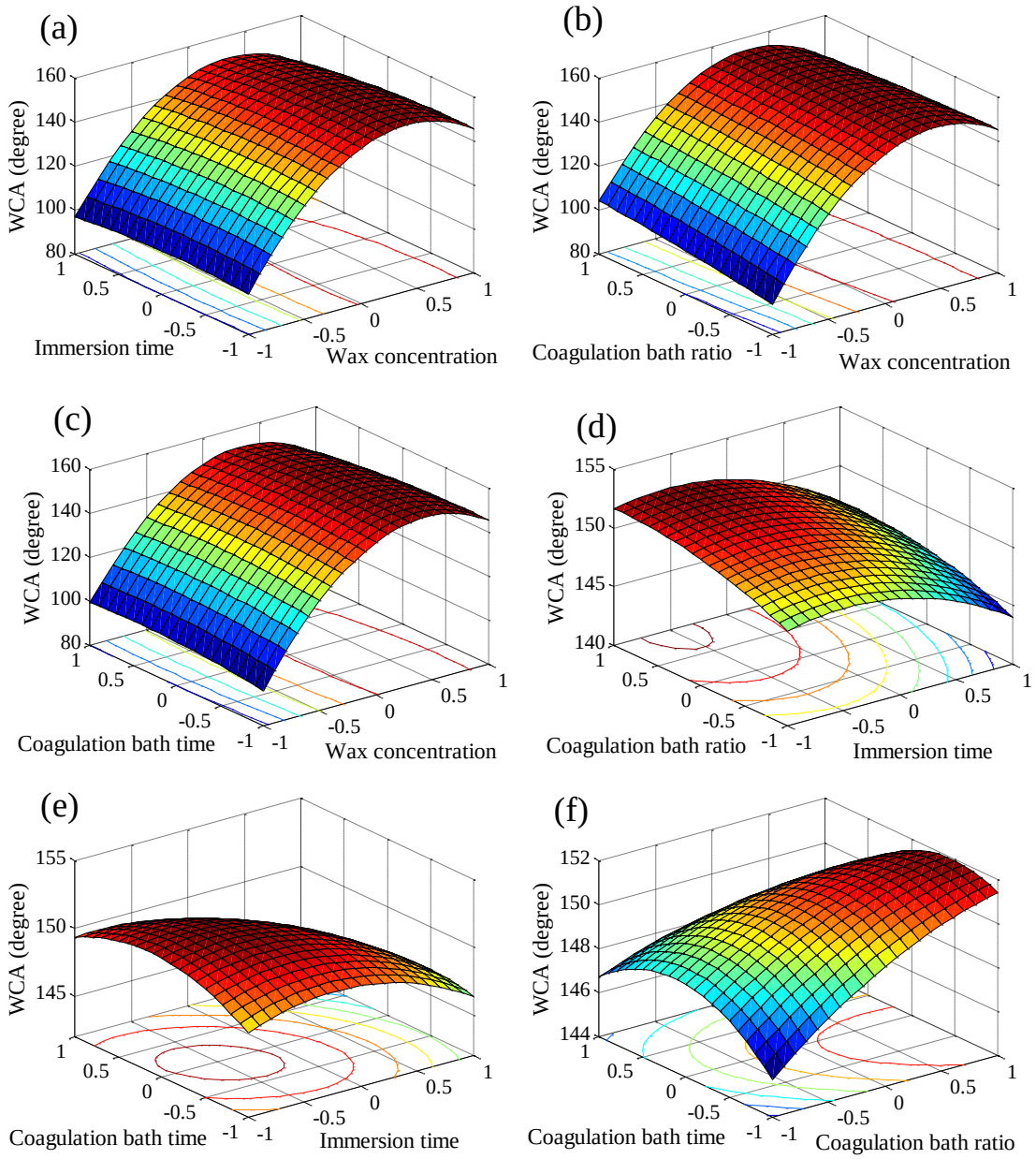

Fig. 2. Response surface plots and corresponding contour plots showing the effects of the interaction between carnauba wax concentration, immersion time, coagulation bath ratio, and coagulation bath time on paper WCA

To evaluate the interactions of the variables and to determine the optimal level of each variable for the maximum response, the response surface analyses were plotted. The obtained three-dimensional response surfaces and two-dimensional contours are shown in Fig. 2. Each figure shows the effect of two variables on paper WCA, while the remaining variables were kept at the zero level. The optimum conditions for paper WCA were as follows: carnauba wax concentration, 3.78% (w/v); immersion time, 1.46 h; coagulation

bath ratio, 13/87 (v/v); and coagulation bath time, 2.63 h, respectively. Accordingly, the theoretical highest paper WCA was predicted as 154.1°.

Table 4. Analysis of Quadratic Regression Equation Coefficients

Variable	Estimated Coefficients	Standard Deviation	*T*-value	*P*-value	Significance
Constant	150.757	0.8862	170.120	0.000	**
X_1	22.194	0.4431	50.090	0.000	**
X_2	-2.188	0.4431	-4.939	0.000	**
X_3	1.636	0.4431	3.692	0.003	**
X_4	-0.695	0.4431	-1.569	0.143	
X_1^2	-28.725	0.6646	-43.220	0.000	**
X_2^2	-2.169	0.6646	-3.264	0.007	**
X_3^1	-0.900	0.6646	-1.355	0.200	
X_4^1	-1.997	0.6646	-3.004	0.011	*
X_1X_2	-1.403	0.7675	-1.827	0.093	
X_1X_3	-3.570	0.7675	-4.652	0.001	**
X_1X_4	-2.420	0.7675	-3.153	0.008	**
X_2X_3	-0.143	0.7675	-0.186	0.856	
X_2X_4	-1.260	0.7675	-1.642	0.127	
X_3X_4	-1.200	0.7675	-1.564	0.144	

**Significant at $P < 0.01$; * Significant at $P < 0.05$.

Validation of the Model

To validate the adequacy of the model equations, a verification experiment was performed according to the optimal conditions mentioned above. Under the optimal conditions, the paper WCA obtained from real experiments was 152.7°, which was consistent with the predicted value of 154.1°. The differences between 152.7° and 154.1° were not significant ($P > 0.05$), which confirmed that the model was accurate and adequate to reflect the expected optimization.

Surface Morphology of Obtained Superhydrophobic Paper

The changes in the morphological structure of the paper surface treated using the phase separation method were confirmed by SEM (Fig. 3).

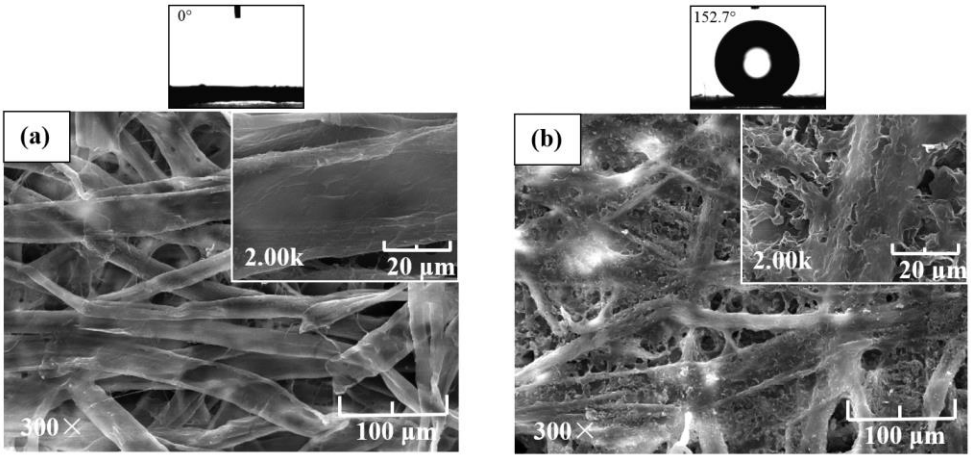

Fig. 3. SEM images of (a) original paper and (b) obtained superhydrophobic paper. The insets correspond to high-magnification SEM images. The top images are representative images of 3 μL water droplets over the surfaces.

The original paper was composed of smooth cellulose fibers, as can be seen in Fig. 3a. Carnauba wax, dissolved in chloroform, was put in contact with the paper surface, where it penetrated the randomly organized cellulose fibers. When it was immersed into the coagulation bath, the non-solvent started to diffuse into the polymer solution. As ethanol and chloroform are miscible, the exchanges between solvent and non-solvent beyond the paper surface resulted in the thermodynamic instability of the system (Zhang *et al*. 2008; Sousa and Mano 2013). To attain the minimum Gibb's free energy, the phase separation of the carnauba wax resulted, separating the wax-poor and wax-rich phases (Sousa and Mano 2013). As can be seen in Fig. 3b, the cluster-like carnauba wax completely covered the fiber surface, forming particularly rough structures. This effect indicated that precipitation of carnauba wax in the wax-poor phase resulted in the dispersion of polymer nuclei, and the precipitation of carnauba wax during the wax-rich phase aggregated around these nuclei, forming the polymer matrix (Aruna *et al.* 2012).

AFM was employed to further investigate the surface ultrastructure and roughness of the obtained superhydrophobic paper. The AFM 3D topographical images are shown in Fig. 4. The original cellulose fiber surface consisted entirely of regularly ordered microfibrils and exhibited a relatively flat topography with a root-mean-square (RMS) roughness of about 7.86 nm (Fig. 4a). When the carnauba wax was precipitated on the cellulose fiber surface by phase separation (Fig. 4b), many cluster-like wax formations developed on the fiber surface, causing a relatively rough topography with an RMS roughness of 25.19 nm. This effect was crucial to generating a superhydrophobic surface, because it is well know that combining appropriate surface roughness with low surface energy materials (hydrophobic carnauba wax in this study) lead to superhydrophobic surface.

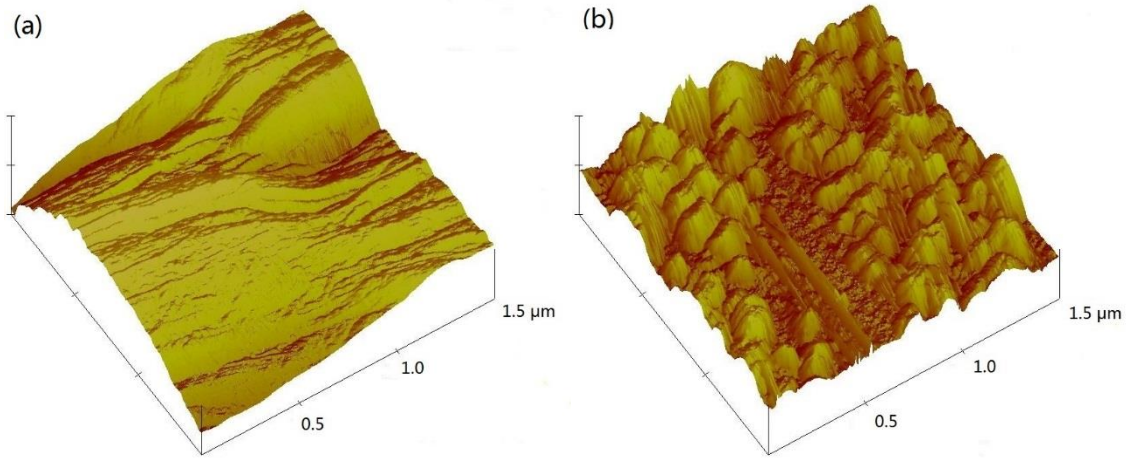

Fig. 4. AFM 3D topographical images of (a) original cellulose fibers and (b) resulting superhydrophobic cellulose fibers

Moisture Resistance Testing

Common natural hydrophobic lipids, such as long-chain fatty acid and waxes used for paper coating, are effective barriers to water or water vapor (Zhang *et al*. 2014). The moisture resistance of the superhydrophobic paper was evaluated by measuring the moisture content and tensile strength of paper specimens at different relative humidities (Figs. 5 and 6). The moisture content (MC) of the sample was calculated using Eq. 2,

$$\text{MC}(\%) = \frac{\text{weight of specimen - weight of dry specimen}}{\text{weight of dry specimen}} \quad (2)$$

where the weight of the dry specimen was obtained by drying a paper specimen at 105 °C until a constant weight was obtained. The relative moisture content (RMC) of the specimen was calculated using Eq. 3:

$$\text{RMC}(\%) = \frac{\text{MC of specimen}}{\text{MC of specimen under 25\% relative humidity}} \quad (3)$$

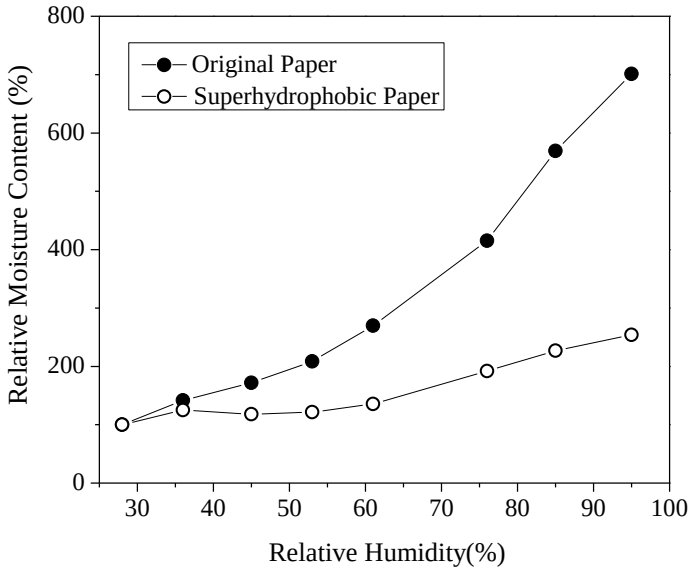

Fig. 5. Relative moisture content *vs*. relative humidity of original and obtained superhydrophobic paper.

As shown in Fig. 5, the relative moisture content of the original paper specimen increased to 701% when the relative humidity increased from 25% to 95%. Compared with the original specimen, the superhydrophobic specimen exhibited much higher moisture resistance; the relative moisture content of the superhydrophobic specimen only increased to 254%. The tensile strengths of the specimens were also measured after they had been conditioned at ambient temperature under different relative humidities for 24 h. The relative tensile strength (TS) of the specimens was calculated using Eq. 4:

$$\text{Relative TS}(\%) = \frac{\text{TS of specimen}}{\text{TS of specimen under 25\% relative humidity}} \quad (4)$$

The relative tensile strength of the original paper specimens decreased obviously under the high relative humidity condition (Fig. 6). Due to the high moisture resistance property, the relative tensile strength of the obtained superhydrophobic specimen showed a slight decreasing trend. These results indicated that the fiber-fiber binding bonds in the paper specimen were protected by the precipitated carnauba wax coating on the cellulose fiber surface. Therefore, the resulting superhydrophobic paper has potential applications in liquid packaging or moisture-proof paper packaging.

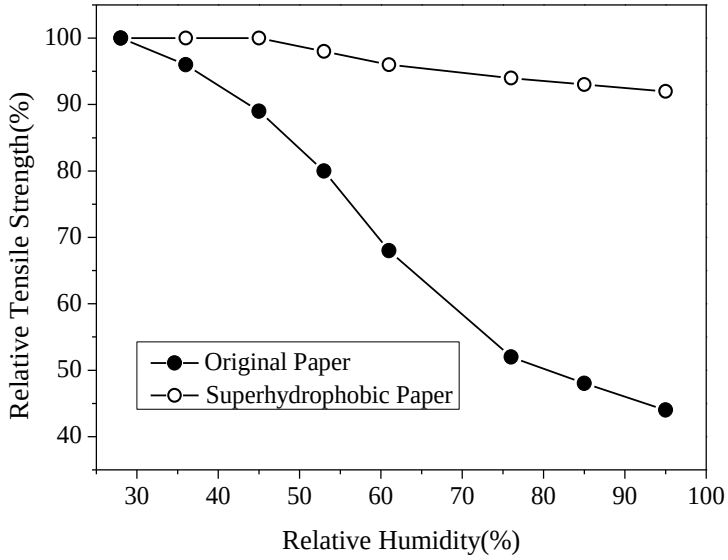

Fig. 6. Relative tensile strength *vs*. relative humidity of original and superhydrophobic paper

CONCLUSIONS

1. Superhydrophobic paper with excellent moisture resistance was prepared by precipitating carnauba wax onto the surface of cellulose fibers using a simple phase separation method.
2. Response surface methodology was used to optimize the effects of preparation parameters on the water contact angle of the paper surface, and the optimal preparation conditions were as follows: carnauba wax concentration ratio, 3.78% (w/v); immersion time, 1.46 h; coagulation bath ratio, 13/87 (v/v); and coagulation bath time, 2.63 h. Under the optimal conditions, the obtained paper surface showed superhydrophobic properties, including a water contact angle of 152.7°.
3. The SEM and AFM images showed that during phase separation, precipitation caused the fiber surface to be covered with cluster-like formations of carnauba wax, which increased the surface RMS roughness of the cellulose fibers.
4. The moisture resistance testing results showed that the obtained superhydrophobic paper had high moisture resistance properties and retained a high tensile strength at conditions of relatively high humidity.

ACKNOWLEDGEMENTS

This work was financially supported by the National Natural Science Foundation of China (No. 21566020), the Applied Basic Research Program of Yunnan Province (No. 2014FD008), and the Talent Training Program of Yunnan Province (No. KKSY201305002).

REFERENCES CITED

Aruna, S. T., Binsy, P., Edna, R., and Basu, B. (2012). "Properties of phase separation method synthesized superhydrophobic polystyrene films," *Appl. Surf. Sci.* 258(7), 3202-3207. DOI: 10.1016/j.apsusc.2011.11.064

Balu, B., Breedveld, V., and Hess, D. W. (2008). "Fabrication of 'roll-off' and 'sticky' superhydrophobic cellulose surfaces *via* plasma processing," *Langmuir* 24(9), 4785-4790. DOI: 10.1021/la703766c

Barman, K., Asrey, R., and Pal, R. K. (2011). "Putrescine and carnauba wax pretreatments alleviate chilling injury, enhance shelf life and preserve pomegranate fruit quality during cold storage," *Sci. Hortic-amsterdam* 130(4), 795-800. DOI: 10.1016/j.scienta.2011.09.005

Bongiovanni, R., Marchi, S., Zeno, E., Pollicino, A., and Thomas, R. R. (2013). "Water resistance improvement of filter paper by a UV-grafting modification with a fluoromonomer," *Colloids Surf. A* 418, 52-59. DOI: 10.1016/j.colsurfa.2012.11.003

Crick, C. R., Bear, J. C., Kafizas, A., and Parkin, I. P. (2012). "Superhydrophobic photocatalytic surfaces through direct incorporation of titania nanoparticles into a polymer matrix by aerosol assisted chemical vapor deposition," *Adv. Mater.* 24(26), 3505-3508. DOI: 10.1002/adma.201201239

Elsharkawy, M., Schutzius, T. M., and Megaridis, C. M. (2014). "Inkjet patterned superhydrophobic paper for open-air surface microfluidic devices," *Lab Chip* 14, 1168-1175. DOI: 10.1039/C3LC51248G

Geissler, A., Loyal, F., Biesalski, M., and Zhang, K. (2014). "Thermo-responsive superhydrophobic paper using nanostructured cellulose stearoyl ester," *Cellulose* 21(1), 357-366. DOI: 10.1007/s10570-013-0160-8

Huang, L. H., Chen, K. F., Lin, C. X., Yang, R. D., and Gerhardt, R. A. (2011). "Fabrication and characterization of superhydrophobic high opacity paper with titanium dioxide nanoparticles," *J. Mater. Sci.* 46(8), 2600-2605. DOI: 10.1007/s10853-010-5112-1

Li, Z. X., Xing, Y. J., and Dai, J. J. (2008). "Superhydrophobic surfaces prepared from water glass and non-fluorinated alkylsilane on cotton substrates," *Appl. Surf. Sci.* 254(7), 2131-2135. DOI: 10.1016/j.apsusc.2007.08.083

Obeso, C. G., Sousa, M. P., Song, W. L., Rodriguez-Pérez, M. A., Bhushan, B., and Mano, J. F. (2013). "Modification of paper using polyhydroxybutyrate to obtain biomimetic superhydrophobic substrates," *Colloids Surf. A* 416, 51-55. DOI: 10.1016/j.colsurfa.2012.09.052

Ogihara, H., Xie, J., Okagaki, J., and Saji, T. (2012). "Simple method for preparing superhydrophobic paper: Spray-deposited hydrophobic silica nanoparticle coatings exhibit high water-repellency and transparency," *Langmuir* 28(10), 4605-4608. DOI: 10.1021/la204492q

Oliveira, N. M., Neto, A. I., Song, W. L., and Mano, J. F. (2010). "Two-dimensional open microfluidic devices by tuning the wettability on patterned superhydrophobic polymeric surface," *Appl. Phys. Express* 3(8), 1-6. DOI: 10.1143/APEX.3.085205

Pradella, J. G., Lenczak, J. L., Delgado, C. R., and Taciro, M. K. (2012). "Carbon source pulsed feeding to attain high yield and high productivity in poly(3-hydroxybutyrate) (PHB) production from soybean oil using *Cupriavidus necator*," *Biotechnol. Lett.* 34(6), 1003-1007. DOI: 10.1007/s10529-012-0863-1

Shi, Y. L., Wang, Y. S., Feng, X. J., Yue, G. R., and Yang, W. (2012). "Fabrication of superhydrophobicity on cotton fabric by sol-gel," *Appl. Surf. Sci.* 258(20), 8134-8138. DOI: 10.1016/j.apsusc.2012.05.008

Sousa, M. P., and Mano, J. F. (2013). "Superhydrophobic paper in the development of disposable labware and lab-on-paper devices," *ACS Appl. Mater. Interface* 5(9), 3731-3737. DOI: 10.1021/am400343n

Tang, X. D., Nan, S. Q., Wang, T. S., Chen, Y., Yu, F. Q., Zhang, G. Y., and Pei, M. S. (2013). "Facile strategy for fabrication of transparent superhydrophobic coatings on the surface of paper," *RSC Adv.* 3, 15571-15575. DOI: 10.1039/C3RA41907J

Werner, O., Quan, C., Turner, C., Pettersson, B., and Wågberg, L. (2010). "Properties of superhydrophobic paper treated with rapid expansion of supercritical CO_2 containing a crystallizing wax," *Cellulose*, 17(1), 187-198. DOI: 10.1007/s10570-009-9374-1

Witte, P., Dijkstra, P. J., Berg, J. W. A., and Feijen J. (1996). "Phase separation processes in polymer solutions in relation to membrane formation," *J. Membr. Sci.* 117(1-2), 1-31. DOI: 10.1016/0376-7388(96)00088-9

Yang, H., and Deng, Y. L (2008). "Preparation and physical properties of superhydrophobic papers," *J. Colloid Interface Sci.* 325(2), 588-593. DOI: 10.1016/j.jcis.2008.06.034

Yuan, Z. Q., Chen, H., Tang, J. X., Chen, X., Zhao, D. J., and Wang, Z. X. (2007). "Facile method to fabricate stable superhydrophobic polystyrene surface by adding ethanol," *Surf. Coat. Technol.* 201(16-17), 7138-7142. DOI: 10.1016/j.surfcoat.2007.01.021

Zhang, L. B., Wu, J. B., Hedhili, M. N., Yang, X. L., and Wang, P. (2015). "Inkjet printing for direct micropatterning of a superhydrophobic surface: Toward biomimetic fog harvesting surfaces," *J. Mater. Chem. A* 3, 2844-2852. DOI: 10.1039/C4TA05862C

Zhang, M., Wang, S. L., Wang, C. Y., and Li, J. (2012). "A facile method to fabricate superhydrophobic cotton fabrics," *Appl. Surf. Sci.* 261, 561-566. DOI: 10.1016/j.apsusc.2012.08.055

Zhang, W. W., Xiao, H. N., and Qian, L. Y. (2014). "Enhanced water vapour barrier and grease resistance of paper bilayers-coated with chitosan and beeswax," *Carbohydr. Polym.* 101, 401-406. DOI: 10.1016/j.carbpol.2013.09.097

Zhang, X. Y., Zhao, N., Liang, S. M., Lu, X. Y., Li, X. F., Xie, Q. D., Zhang, X. L., and Xu, J. (2008). "Facile creation of biomimetic systems at the interface and in bulk," *Adv. Mater.* 20(15), 2938-2946. DOI: 10.1002/adma.200800626

Article submitted: March 29, 2016; Peer review completed: June 4, 2016; Revised version received and accepted: June 6, 2016; Published: June 22, 2016.
DOI: 10.15376/biores.11.3.6552-6565